CHAPTER SEVEN

INTERFACIAL ADHESION BETWEEN THE PI/TiO$_2$ NANO HYBRID FILMS AND COPPER SYSTEM

Summary

With the increasing of the use of polymers in the microelectronic industry, adequate adhesion between dissimilar materials is more important. The present investigation attempts to gain an insight into the adhesion mechanism and the related microstructure at the interface between PI/TiO$_2$ hybrid films and copper (Cu). The polymer substrate used in this study is BTDA/ODA-TiO$_2$ nano hybrid films. Moreover, the surface modifications of plasma treatments (Ar, Ar/N$_2$ and Ar/O$_2$) are applied to improve the adhesion strength between PI/TiO$_2$ hybrid films and Cu. The effects of TiO$_2$ content and plasma treatment on adhesion strength and peeled-off failure mode are also investigated in this chapter.
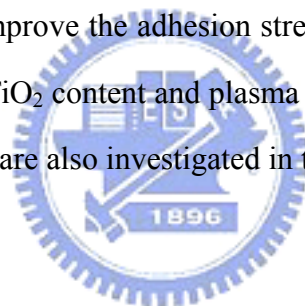
7.1 AFM Analysis

Nanosized TiO$_2$ is incorporated into the BTDA/ODA matrix as the polymer substrate in this study. The changes in surface topography of the PI/TiO$_2$ hybrid films before and after plasma treatment are investigated by atomic force microscopy (AFM). Figure 7.1 shows the AFM images of the pristine PI/TiO$_2$-1wt% hybrid film surface and after plasma modified surface. The root mean square surface roughness (R_a) of the pristine PI/TiO$_2$-1wt% hybrid film is 0.34 nm. After plasma treatment, the surface topography is changed considerably. The R_a values increase to 0.47, 0.54, and 1.1 nm for Ar, Ar/N$_2$ and Ar/O$_2$ plasma treatments, respectively. It is suggested that oxygen is a much more active gas than nitrogen, thus the oxygen plasma is likely to produce rougher surface as compared with nitrogen plasma. As shown in Table 7.1, the similar tendency of increasing

roughness for the other PI/TiO$_2$ hybrid film is observed. Surface roughness is also related with the content of TiO$_2$. The more TiO$_2$ is contained, the more rugged surface is shown and that can facilitate the mechanical interlocking effect during Cu sputtering.
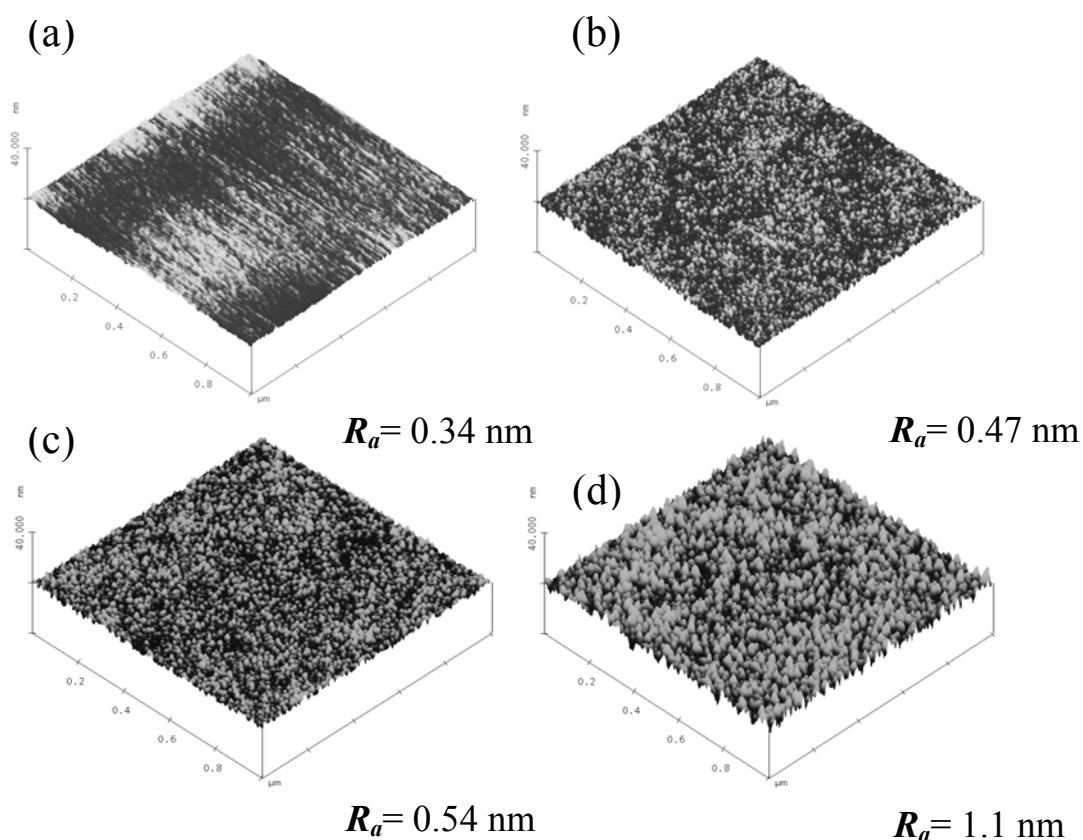
(a) (b)

R_a= 0.34 nm R_a= 0.47 nm

(c) (d)

R_a= 0.54 nm R_a= 1.1 nm

Figure 7.1 AFM images of PI/TiO$_2$-1wt% hybrid film after various plasma treatments. (a) no plasma (b) Ar plasma (c) Ar/N$_2$ plasma (d) Ar/O$_2$ plasma.

Table 7.1 Surface roughness (R_a) of PI/TiO$_2$ hybrid films after plasma treatment.

Plasma treatment	Surface roughness (nm)					
	pure PI	1 wt.%	3 wt.%	5 wt.%	7 wt.%	9 wt.%
No plasma	0.28	0.34	0.38	0.51	0.57	0.63
Ar plasma	0.36	0.47	0.63	0.86	1.56	2.12
Ar/N$_2$ plasma	0.48	0.54	0.82	1.12	1.78	2.34
Ar/O$_2$ plasma	0.71	1.10	1.97	2.46	3.74	4.89

7.2 Surface Energy Analysis

The surface energy and surface roughness of PI/TiO$_2$-1wt% hybrid film after plasma treatment are plotted in Figure 7.2. The pristine hybrid film (no plasma treatment) shows a low surface energy value, indicating a poor wettability. However, the plasma-treated surface produces a noticeable increase in surface energy (i.e. high wettability) and the surface energy values are close, no matter what kind of plasma is used. As shown in Table 7.2, the surface energies of pure polyimide and PI/TiO$_2$ hybrid films with various TiO$_2$ content without plasma treatment are in the range of 31.11~36.33 dy/cm. Once using plasma treatment, the surface energies of pure polyimide and all PI/TiO$_2$ hybrid films vary from 60.63 to 72.2 dy/cm. The changes in surface energy after plasma treatment could be ascribed to the modifications of surface roughness and surface chemistry [1-5]. Besides, it should be noted that the hybrid film surface after plasma treatment by RF generator is not exactly represented the one during Cu sputtering because the process of Cu sputtering is always accompanied by Ar plasma treatment with DC power. Therefore, 〝no plasma〞 sample for contact angle and AFM measurements is different from 〝no plasma〞 sample for adhesion test. To distinguish one from the other, we assumes that the sample without plasma treatment by RF is regarded as 〝no plasma〞 sample in this study.

Table 7.2 Surface energies of various PI/TiO$_2$ hybrid films with different plasma treatments.

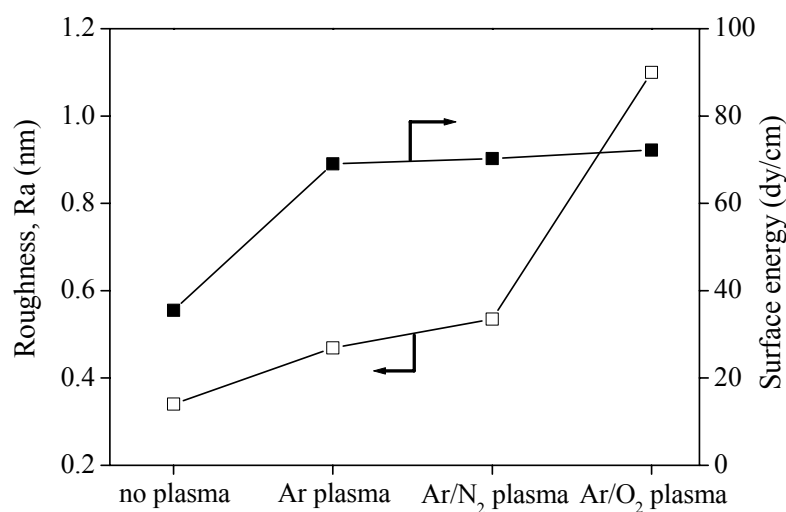| Plasma treatment	Surface energy (dy/cm)					
	pure PI	1 wt%	3 wt%	5 wt%	7 wt%	9 wt%
No plasma	33.20	35.51	35.06	36.33	33.81	31.11
Ar plasma	60.63	70.26	68.74	69.46	70.55	70.30
Ar/N$_2$ plasma	65.56	69.05	69.82	71.59	71.71	71.66
Ar/O$_2$ plasma	68.79	72.20	71.78	71.21	71.31	69.94

Figure 7.2 The surface roughness and surface energy of PI/TiO$_2$-1wt% hybrid film after various plasma treatments.

7.3 Peel Strength Analysis

The peel strength between the PI/TiO$_2$ hybrid films and Cu is estimated by 90° peel tests to investigate the effects of nanosized TiO$_2$ content and plasma treatment. Figure 7.3 represents the peel strength between the PI/TiO$_2$ hybrid films and Cu under various plasma treatments. The peel strength of the hybrid films without plasma treatment is below 1.5 N/cm, while the peel strength of the Ar plasma-treated hybrid films is in the range of 2.6-6.97 N/cm. The Ar/N$_2$ and Ar/O$_2$ plasma treatments are much more effective in promoting the peel strength. In particular, the Ar/N$_2$ treatment causes a large increase in the peel strength from 2.78 to 9.53 N/cm. The peel strength is increased about ten-fold compared with pristine PI (0.86 N/cm).

A tendency that the peel strength can be greatly improved by adding small amounts of TiO$_2$ could result from the existence of TiO$_2$ on the hybrid films surface which reduces the surface resistivity of the hybrid films [6-8]. The more

TiO_2 is contained on the hybrid films surface, the higher conductivity is expected and it becomes easier for Cu to adhere to the hybrid films. However, for the hybrid films with high TiO_2 content, the sample delaminates within the polymer substrate, not at the interface or in the Cu layer during the peel test. This is resulted from the incorporation of TiO_2 into the polyimide matrix causes a loss in flexibility of the hybrid films. Therefore, the mobility of polymer chains is diminished, and the hybrid films with high TiO_2 content are embrittled. For this reason, the hybrid films with high TiO_2 content are too brittle to withstand larger load without fracture during the peel test.
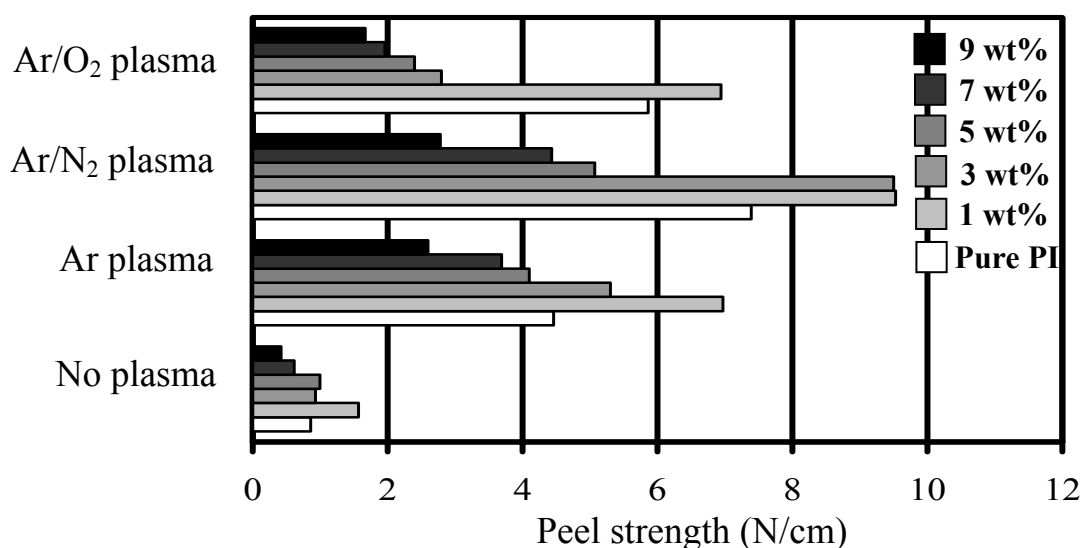
Figure 7.3 The peel strengths between the PI/TiO_2 hybrid films and Cu.

According to Figure 7.3, another factor involved in peel strength is plasma treatment, which can affect the peel strength in three ways. First, the plasma treatment may change the surface morphology to provide mechanical interlocking between the PI/TiO_2 hybrid films and Cu. Second, the TiO_2 content on the hybrid films surface increases after plasma treatment. Third, the plasma treatment may chemically modify the PI/TiO_2 hybrid films surface to form functional groups which ensure either chemical or physical bonds between the hybrid films and Cu

[9-13]. It is reported that active gases plasma (O_2 and N_2) are used to increase the number of N– or O–containing functional groups such as C–O, C–N, C=O and OH at the polyimide surface [14-16]. Since metal atoms preferentially react with C–O, C–N or C=O, the interaction of such groups with Cu and/or Ti atoms is thought to have occurred at the interface. However, when an inert Ar gas is used for the surface treatment, the formation of N– or O–containing groups does not occur easily. This implies the chemical interaction at the hybrid film and Cu interface becomes weak. This is why the lower peel strength is observed for Ar plasma treatment as compared with Ar/N_2 and Ar/O_2 plasma treatments.

7.4 XPS and SEM Analysis

The XPS analyses of PI/TiO_2 hybrid films (see Table 7.3) are consistent with that mentioned above. The plasma treatment leads to a large increase in the [O]/[C] atomic ratio but a smaller increase in the [N]/[C] atomic ratio. The [O]/[C] atomic ratio increases from 0.222 for the untreated hybrid film to 0.5-0.622 for the plasma-treated hybrid films. On the other hand, the [N]/[C] atomic ratio is 0.04 for the untreated hybrid films and 0.041~0.054 for the plasma-treated hybrid films. The correlation between the increase of [O]/[C] and [N]/[C] ratios and increase of adhesion strength is observed. The Ar/O_2 plasma treatment shows similar atomic ratios with Ar/N_2 plasma treatment, but poor adhesion. It is suggested that the degradation (bond scission of imide rings) of hybrid film in the Ar/O_2 plasma may be more intense than Ar and Ar/N_2 plasma. As a result, the Ar/O_2 plasma-treated hybrid films surface easily contains a weak boundary which hampers adhesion [17-18]. We believe that the improvement in adhesion could be attributed to a combination of the lower surface resistivity resulted by incorporating TiO_2 and the plasma treatment.

Table 7.3 The component percentages and atomic ratios of PI/TiO$_2$-9 wt% hybrid films after various plasma treatments.

Plasma treatment	component percentage (%)				atomic ratio		
	C	N	O	Ti	[O]/[C]	[N]/[C]	[O]/[N]
No plasma	78.78	3.22	17.48	0.52	0.222	0.040	5.429
Ar plasma	61.17	2.53	30.6	5.7	0.500	0.041	12.095
Ar/N$_2$ plasma	54.98	2.99	33.34	8.69	0.606	0.054	11.151
Ar/O$_2$ plasma	54.67	2.62	33.98	8.73	0.622	0.048	12.969

To investigate the interfacial state, XPS spectra of the PI/TiO$_2$ hybrid film surfaces that had been modified by various plasma treatments after peel test are shown in Figure 7.4. For PI/TiO$_2$-9 wt% hybrid film, the apparent Cu peaks are only observed in Figure 7.4 (d) when hybrid film is activated by Ar/O$_2$ plasma treatment. No Cu signal is detected for the other three plasma treatments. In order to understand this point, two represented plasma treatments (Ar/N$_2$ and Ar/O$_2$) are chosen and both surfaces of the hybrid film peeled from the Cu, and the surface of the Cu are analyzed by XPS and SEM.
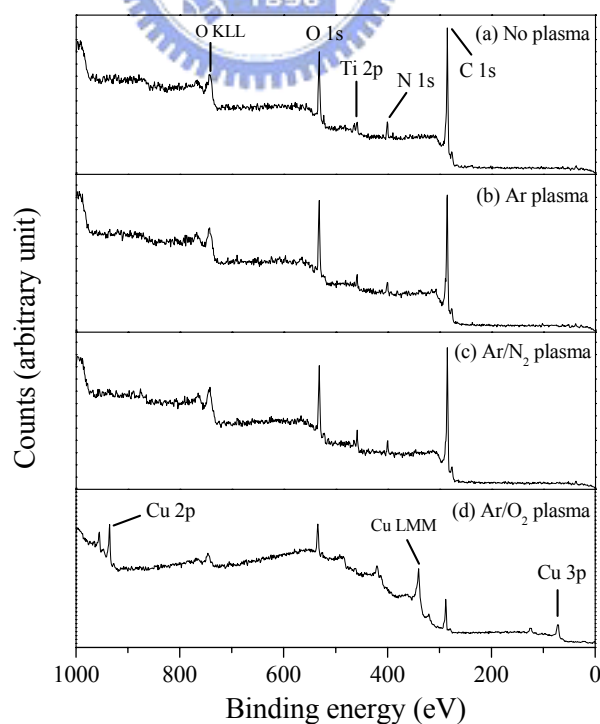

Figure 7.4 XPS spectra of PI/TiO$_2$-9 wt% hybrid films surface treated with various plasma treatments after peel test.

In this study, the failed surface obtained after peel test are identified as polymer side (the surface which corresponds to the hybrid film) and Cu side (the surface adhered to hybrid film). Figure 7.5 presents the XPS spectra of both polymer side and Cu side modified by Ar/N$_2$ plasma treatment. The Cu 2p$_{3/2}$ (933 eV) peaks can be seen in the spectrum of polymer side as well as on the Cu side for pure polyimide (without TiO$_2$ additive) [19-20]. This result suggests that some polyimide is transferred to the Cu side and some Cu diffuse to the polyimide surface. In contrast, with TiO$_2$ additive, the XPS analyses of the peeled-off PI/TiO$_2$ hybrid films show no signal of Cu. Therefore, it can be inferred that the peeled-off failure mode of pure PI−Cu system is different from that of PI/TiO$_2$ hybrid film−Cu system. When polyimide surface is activated by Ar/N$_2$ plasma treatment, the failure locus of the pure PI−Cu system is at the interphase layer. While for the PI/TiO$_2$ hybrid film−Cu system, cohesive failure occurs in the inner layer of hybrid films.

Figure 7.6 is the SEM image showing the morphology of peeled-off polymer side modified by Ar/N$_2$ plasma treatment. Except for pure PI, where a smooth surface is presented, a distinctly lumpy surface is seen for PI/TiO$_2$ hybrid film. In particular the images of PI/TiO$_2$-1 wt% (Ar/N$_2$) and PI/TiO$_2$-3 wt% (Ar/N$_2$), for which the stronger peel strengths are obtained, show significantly peeled-off deformation structure (Figure 7.6 (b) and (c)). In the case of PI/TiO$_2$-9 wt% (Ar/N$_2$), it displays another type of surface failure. Figure 7.6 (d) shows very regular period of failure. The long periodic deformation on the surface could be due to its relative rigidity. High rigidity leads the hybrid film to not easily undergo plastic deformation during the peel test. Instead, it accumulates the energy until the critical value and the fail occurs. It is believed that some kind of correlation between the content of TiO$_2$ and the interface adhesion mechanism results in the distinct difference of peeled-off morphology.
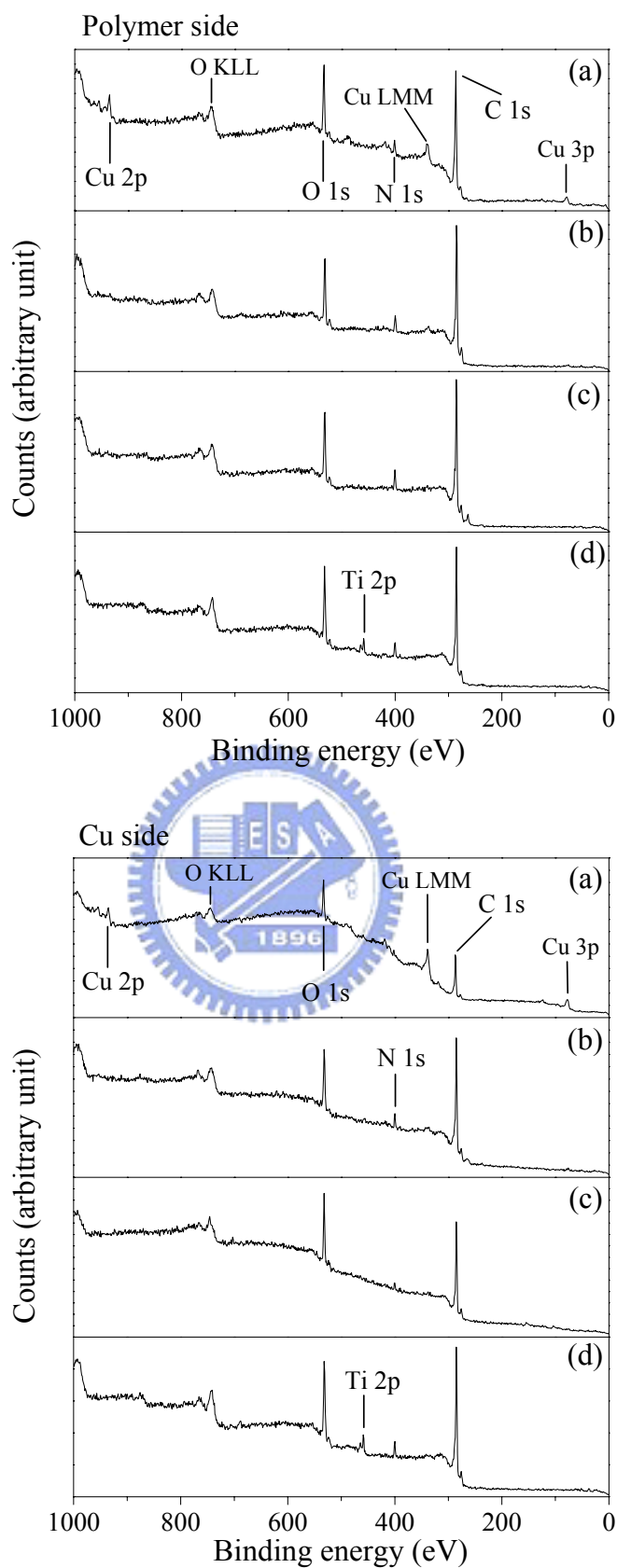
Figure 7.5 XPS spectra of both polymer side and Cu side with Ar/N$_2$ plasma treatment (a) pure PI (b) PI/TiO$_2$-1 wt% (c) PI/TiO$_2$-3 wt% (d) PI/TiO$_2$-9 wt%.
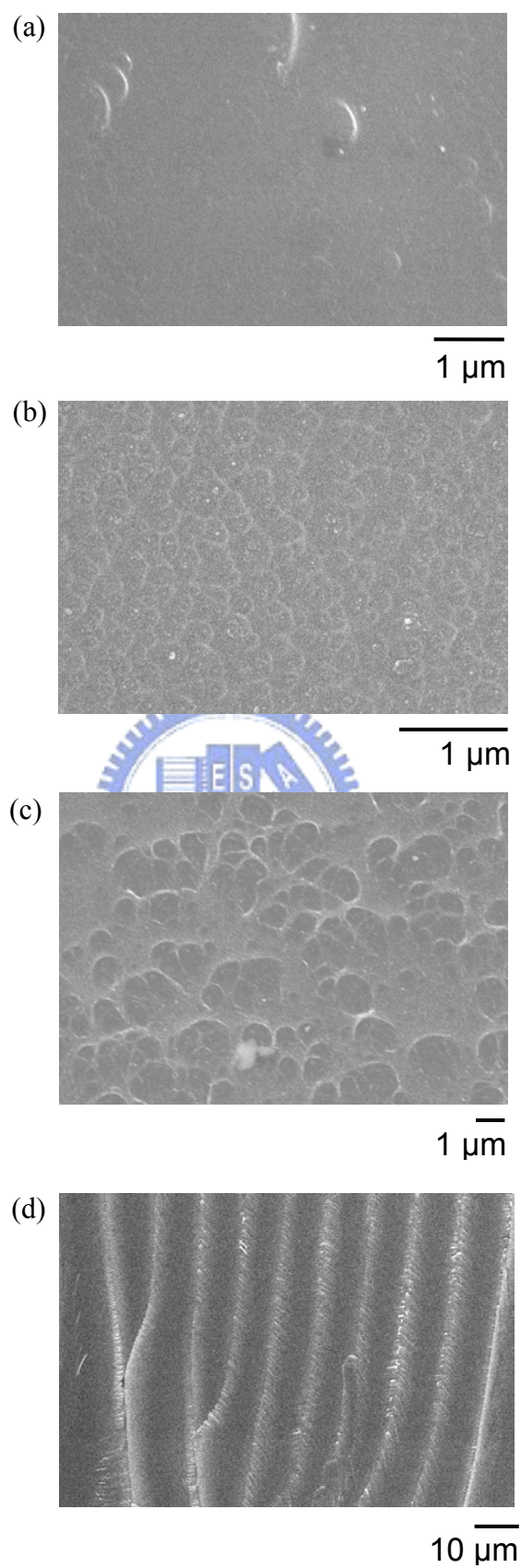
(a)

1 µm

(b)

1 µm

(c)

1 µm

(d)

10 µm

Figure 7.6 SEM images of peeled-off surface of hybrid film with Ar/N$_2$ plasma treatment (a) pure PI (b) PI/TiO$_2$-1 wt% (c) PI/TiO$_2$-3 wt% (d) PI/TiO$_2$-9 wt%.

The effect of Ar/O$_2$ plasma treatment on interfacial state is also examined by XPS and SEM. Figure 7.7 shows the XPS spectra of polymer and Cu sides for the PI/TiO$_2$ hybrid film that had been subjected to Ar/O$_2$ plasma treatment. In Figure 7.7, a distinct peak at the binding energy of 935 eV, attributable to the CuO species [20-21], is discernible in the spectra of polymer side (Figure 7.7 (c) and (d)) and Cu side (Figure 7.7 (a) and (b)). The existence of CuO could be due to the fact that the copper oxide is formed at the interface region during Cu sputtering. It is believed that the interface consists of copper oxide is a weak boundary. When the peel test is carried out, the interface of plasma treated region fails easily. For this reason, the hybrid films treated with Ar/O$_2$ plasma produce poorer adhesion strength than that treated with Ar/N$_2$ plasma.
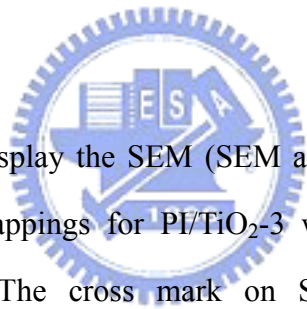
According to Figure 7.7, no obvious Cu signal is detected on polymer side (Figure 7.7 (a) and (b)) for pure PI (Ar/O$_2$) and PI/TiO$_2$-1 wt% (Ar/O$_2$), even when TiO$_2$ is incorporated in the latter. Taking the AFM results into account, the more TiO$_2$ is incorporated, the rougher the PI/TiO$_2$ hybrid film surface that is observed after plasma treatment. The roughness provides an easy way for Cu to diffuse into the polymer side. Hence, pure PI and PI/TiO$_2$-1 wt% with only slight surface roughness restrict the motion of Cu into polymer layer. That is why Cu peak is only found from the Cu side for pure PI (Ar/O$_2$) and PI/TiO$_2$-1 wt% (Ar/O$_2$).

On the other hand, in the cases of PI/TiO$_2$-3 wt% (Ar/O$_2$) and PI/TiO$_2$-9 wt% (Ar/O$_2$), the more rugged surface facilitates the diffusion of Cu into the hybrid film and the Cu signal is detected from the polymer side. The peeled-off failure mode of pure PI (Ar/O$_2$) and PI/TiO$_2$-1 wt% (Ar/O$_2$) is at the interfacial of hybrid films and Cu due to Cu signal is only found in Cu side. However, for PI/TiO$_2$-3 wt% (Ar/O$_2$) and PI/TiO$_2$-9 wt% (Ar/O$_2$), the Cu signal is only detected on the polymer side, suggesting that the failure locus is shifted to the inner interphase between the

PI/TiO$_2$ hybrid films and Cu.

The SEM images of the peeled-off polymer side modified by Ar/O$_2$ plasma treatment are presented in Figure 7.8. The morphology of pure PI (Ar/O$_2$) and PI/TiO$_2$-1 wt% (Ar/O$_2$) show that there are some random islands existing on the peeled-off hybrid film surfaces. With increasing TiO$_2$ content, the structure of multi-level is observed. The result further suggests that not only adhesion strength but also on interfacial state between the hybrid film and Cu is affected by plasma treatment. Besides, the failure mode between the hybrid films and Cu is also related. More work needs to be carried out of how the additive of TiO$_2$ affects the peel strength and the interface adhesion mechanism between the PI/TiO$_2$ hybrid films and Cu.

7.5 EDS Analysis

Figures 7.9 and 7.10 display the SEM (SEM at different magnifications) images and EDS elemental mappings for PI/TiO$_2$-3 wt% (Ar/N$_2$) and PI/TiO$_2$-1 wt% (Ar/O$_2$), respectively. The cross mark on SEM image represents the spot characterized by energy dispersive spectrometer (EDS). The result shows that the hybrid film pre-treated with Ar/O$_2$ plasma has a higher atomic ratio of oxygen to copper as compared with that treated with Ar/N$_2$ plasma. It is suggested that not only copper but also other copper compounds are presented. This is consistent with the XPS observation that copper oxide could be formed during Cu sputtering by Ar/O$_2$ plasma treatment. The presence of gold (Au) is from the Au coating used for SEM sample preparation.
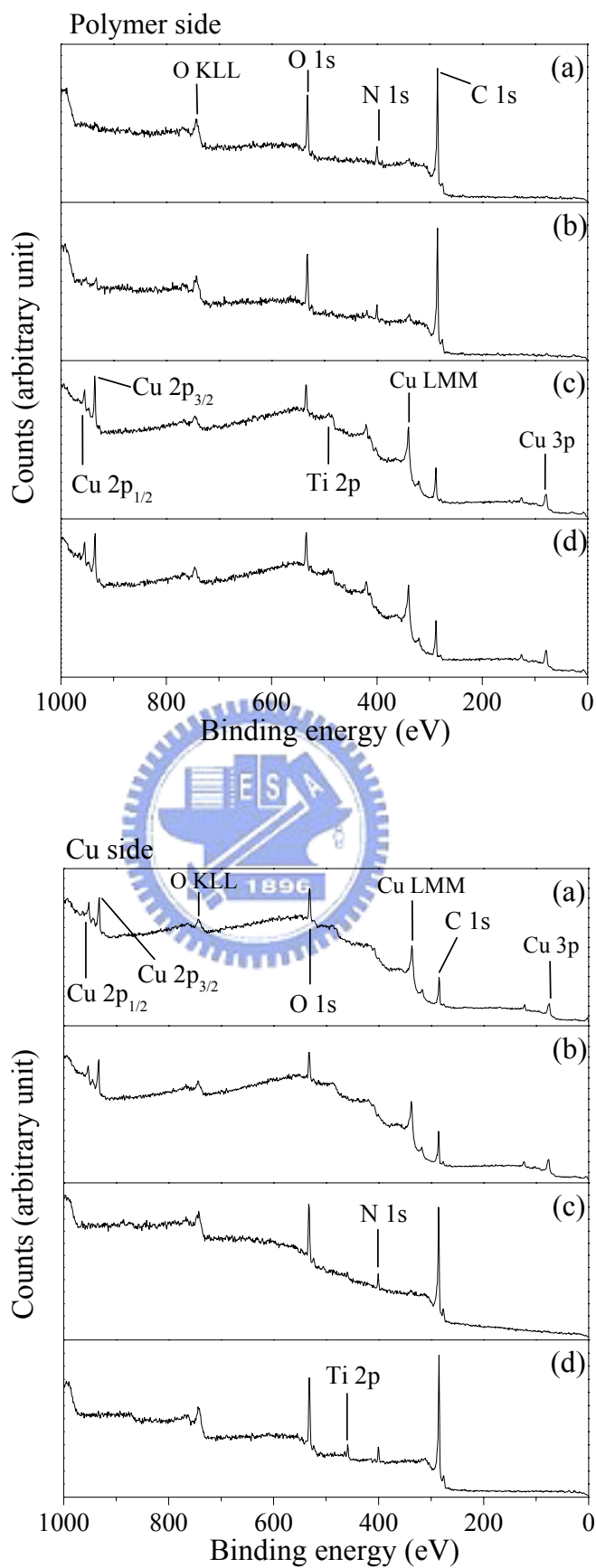
Polymer side

Cu side

Figure 7.7 XPS spectra of both polymer side and Cu side with Ar/O$_2$ plasma treatment (a) pure PI (b) PI/TiO$_2$-1 wt% (c) PI/TiO$_2$-3 wt% (d) PI/TiO$_2$-9 wt%.

(a)

1 μm
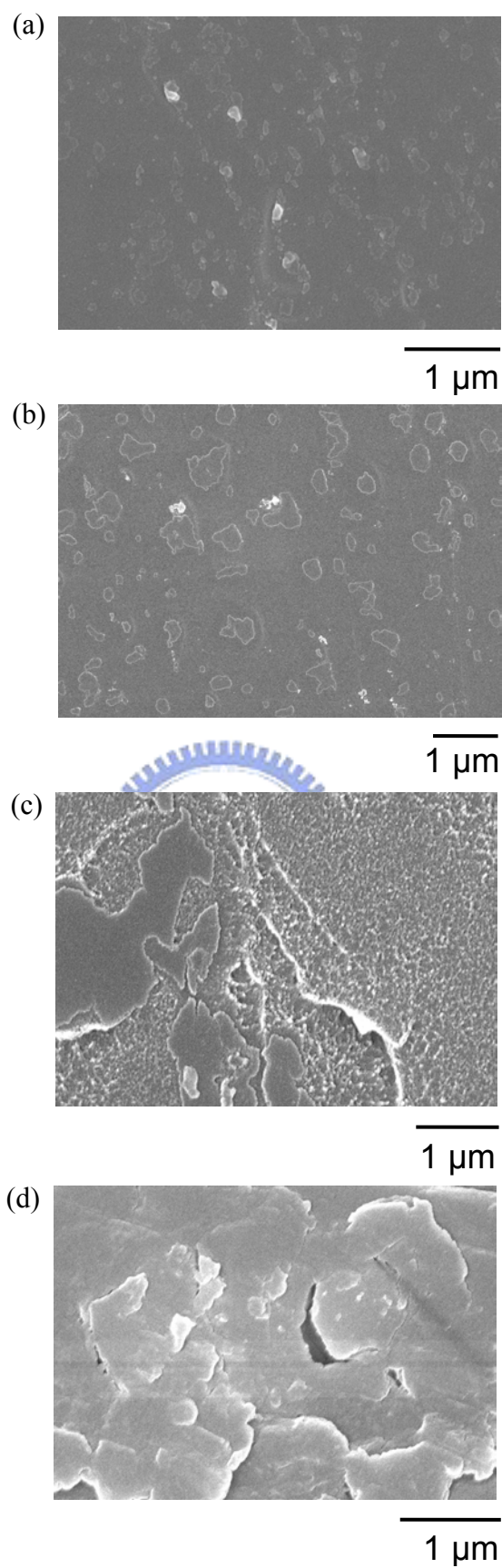
(b)

1 μm

(c)

1 μm

(d)

1 μm

Figure 7.8 SEM images of peeled-off surface of hybrid film with Ar/O$_2$ plasma treatment (a) pure PI (b) PI/TiO$_2$-1 wt% (c) PI/TiO$_2$-3 wt% (d) PI/TiO$_2$-9 wt%.
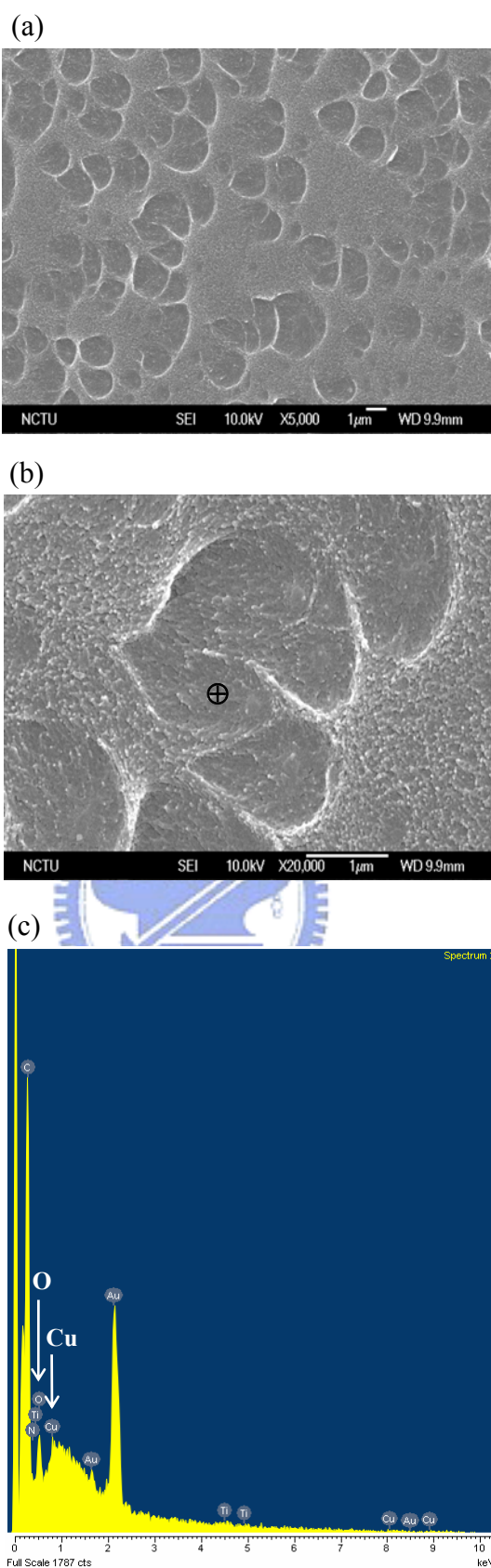
(a)

(b)

(c)

Figure 7.9 PI/TiO$_2$-3 wt% hybrid film with Ar/N$_2$ plasma treatment. (a) SEM image (b) SEM image (c) EDAX mapping.
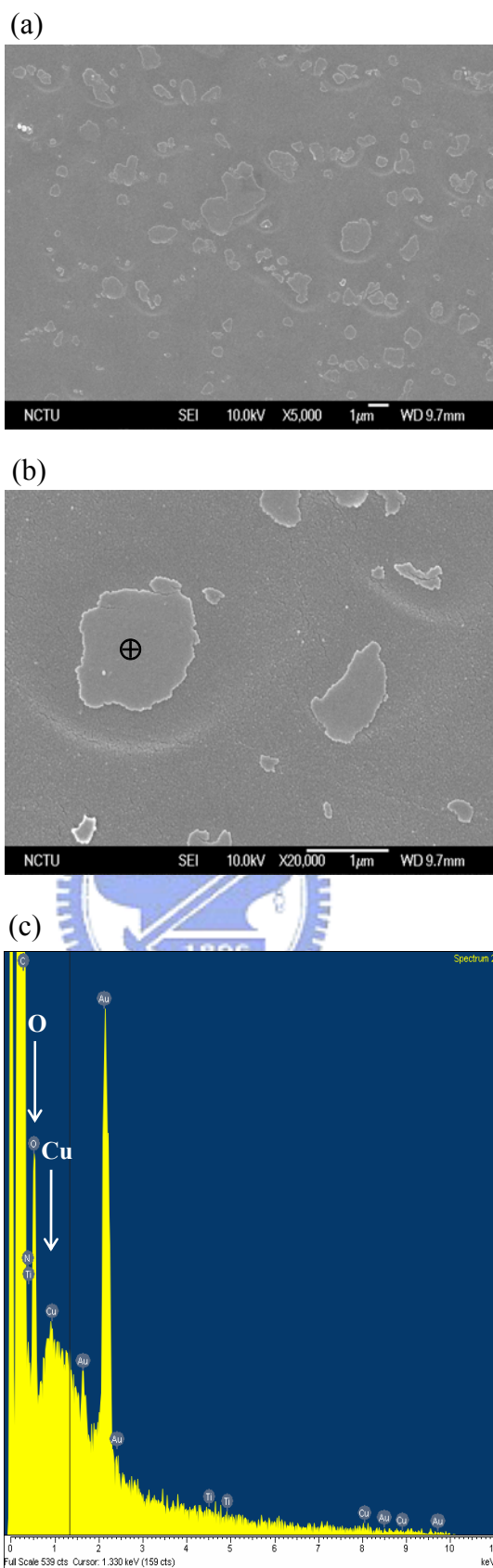
(a)

(b)

(c)

Figure 7.10 PI/TiO$_2$-1 wt% hybrid film with Ar/O$_2$ plasma treatment. (a) SEM image (b) SEM image (c) EDAX mapping.

7.6 Conclusion

Polyimide (PI) containing small amounts of nanosized TiO_2 has significantly enhanced the adhesion strength with Cu. The improvement of adhesion strength could be attributed to the higher conductivity resulted from the existence of TiO_2 on the hybrid film surface. However, further addition of TiO_2 causes a failure or crack within the polymer substrate instead of interfacial failure during the peel test. Owing to the increase of rigidity, the hybrid film is too brittle to afford larger load without fracture. The results of peel tests also indicate the adhesion strength is higher than the mechanical strength of the PI/TiO_2 hybrid film substrate.

Another factor involved in adhesion improvement is the plasma treatment which leads to enhance adhesion between the PI/TiO_2 hybrid films and Cu. The Ar/N_2 plasma treatment is more effective than Ar and Ar/O_2 plasma treatments. The PI/TiO_2-1 wt% hybrid film treated with Ar/N_2 plasma exhibits the maximum adhesion strength of 9.53 N/cm. A correlation between the enhancement of adhesion strength and increasing [O]/[C] and [N]/[C] atomic ratios is observed.

A weak boundary layer of CuO is found at the interface may be the reason why the Ar/O_2 plasma-treated hybrid film shows a poorer adhesion than Ar/N_2 plasma-treated one. In addition, the peeled-off failure mode is also deeply related to the content of TiO_2 and what kind of plasma treatment is used. The locus of failure is shifted from the inner layer of the PI/TiO_2 hybrid film to the interfacial between the hybrid film and Cu by Ar/N_2 and Ar/O_2 plasma treatments, respectively.

7.7 References

1.   N. Inagaki, S. Tasaka, K. Hibi, *J. Adhesion Sci. Technol.* 8(4): 395 (1994).

2.   G. Rozovskis, J. Vinkevicius, J. Jaciauskiene, *J. Adhesion Sci. Technol.* 10(5): 399 (1996).

3. A. M. Ektessabi, S. Hakamata, *Thin Solid Films* 377-378: 621 (2000).

4. M. K. Ghosh, K. L. Mittal eds., *Polyimides: fundamentals and applications* New York (1996).

5. C. Feger, M. M. Khojasteh, J. E. McGrath, *Polyimides: materials, chemistry and characterization* New York, Elsevier (1989).

6. C. A. Chang, J. E. Balgin, A. G. Schrott, K. C. Lin, *Applied Physics Letters* 51: 103 (1987).

7. Y. Nakamura, Y. Suzuki, Y. Watanabe, *Thin Solid Films* 290-291: 367 (1996).

8. P. C. Chiang, W. T. Whang, *Polymer* 44: 2249 (2003).

9. F. S. Ohuchi, S. C. Freilich, *J. Vac. Sci. Technol.* A4: 1039 (1986).

10. L. J. Atanasoska, S. G. Anderson, H. M. Meyer, Z. Lin, J. H. Weaver, *Vac. Sci. Technol.* A5: 3325 (1987).

11. N. J. Chou, C. H. Tang, *J. Vac. Sci. Technol.* A2: 751 (1984).

12. J. L. Jordan, P. N. Sanda, J. F. Morar, C. A. Kovac, F. J. Himpsel, R. A. Pollack, *J. Vac. Sci. Technol.* A4: 1046 (1986).

13. G. S. Chang, K. H. Chae, C. N. Whang, *Applied Physics Letters* 74: 522 (1999).

14. E. Kondoh, *Thin Solid Films* 359: 255 (2000).

15. A. Ebe, E. Takahashi, Y. Iwamoto, N. Kuratani, S. Nishiyama, O. Imai, K. Ogata, Y. Setsuhara, S. Miyake, *Thin Solid Films* 281-282: 356 (1996).

16. K. S. Kim, Y. C. Jang, H. J. Kim, Y. C. Quan, J. Choi, D. Jung, N. E. Lee, *Thin Solid Films* 377-378: 122 (2000).

17. N. Inagaki, S. Tasaka, K. Hibi, *J. Adhesion Sci. Technol.* 8(4): 395 (1994).

18. I. S. Park, E. C. Ahn, *Materials Science and Enginnering* A282: 137 (2000).

19. G. Rozovskis, J. Vinkevicius, *Adhesion Sci. Technol.* 10(5): 399 (1996).

20. A. M. Ektessabi, S. Hakamata, *Thin Solid Films* 377-378: 621 (2000).

21. C. A. Chang, J. E. Balgin, A. G. Schrott, K. C. Lin KC. *Applied Physics Letters* 51: 103 (1987).